

Mechanism of optical absorption enhancement in thin film organic solar cells with plasmonic metal nanoparticles

Di Qu,¹ Fang Liu,^{1,*} Yidong Huang,^{1,2} Wanlu Xie,¹ and Qi Xu¹

¹State Key Laboratory of Integrated Optoelectronics, Department of Electronic Engineering, Tsinghua University, Beijing 100084, China

²yidonghuang@tsinghua.edu.cn

*liu_fang@tsinghua.edu.cn

Abstract: The optical absorption enhancement in thin film organic solar cells (OSCs) with plasmonic metal nanoparticles (NPs) has been studied by means of finite element method with a three-dimension model. It is found that significant plasmonic enhancement of above 100% can be obtained by introducing Ag-NPs at the interface between P3HT:PCBM active layer and PEDOT:PSS anode layer. This enhancement is even larger than that with Ag-NPs totally embedded in the P3HT:PCBM active layer of thin film OSCs. Furthermore, the enhancement mechanism of Ag-NPs at different positions of thin film OSCs is investigated.

©2011 Optical Society of America

OCIS codes: (350.6050) Solar energy; (250.5403) Plasmonics; (310.6805) Theory and design.

References and links

1. H. A. Atwater and A. Polman, "Plasmonics for improved photovoltaic devices," *Nat. Mater.* **9**(3), 205–213 (2010).
2. D. Qu, F. Liu, J. F. Yu, W. L. Xie, Q. Xu, X. D. Li, and Y. D. Huang, "Plasmonic core-shell gold nanoparticle enhanced optical absorption in photovoltaic devices," *Appl. Phys. Lett.* **98**(11), 113119 (2011).
3. S. Pillai, K. R. Catchpole, T. Trupke, and M. A. Green, "Surface plasmon enhanced silicon solar cells," *J. Appl. Phys.* **101**(9), 093105 (2007).
4. S. H. Lim, W. Mar, P. Matheu, D. Derkacs, and E. T. Yu, "Photocurrent spectroscopy of optical absorption enhancement in silicon photodiodes via scattering from surface plasmon polaritons in gold nanoparticles," *J. Appl. Phys.* **101**(10), 104309 (2007).
5. D. Derkacs, S. H. Lim, P. Matheu, W. Mar, and E. T. Yu, "Improved performance of amorphous silicon solar cells via scattering from surface plasmon polaritons in nearby metallic nanoparticles," *Appl. Phys. Lett.* **89**(9), 093103 (2006).
6. K. R. Catchpole and A. Polman, "Plasmonic solar cells," *Opt. Express* **16**(26), 21793–21800 (2008).
7. F. J. Tsai, J. Y. Wang, J. J. Huang, Y. W. Kiang, and C. C. Yang, "Absorption enhancement of an amorphous Si solar cell through surface plasmon-induced scattering with metal nanoparticles," *Opt. Express* **18**(S2 Suppl 2), A207–A220 (2010).
8. M. Yang, Z. P. Fu, F. Lin, and X. Zhu, "Incident angle dependence of absorption enhancement in plasmonic solar cells," *Opt. Express* **19**(S4 Suppl 4), A763–A771 (2011).
9. Y. A. Akimov and W. S. Koh, "Design of plasmonic nanoparticles for efficient subwavelength light trapping in thin-film solar cells," *Plasmonics* **6**(1), 155–161 (2011).
10. Y. A. Akimov, K. Ostrikov, and E. P. Li, "Surface plasmon enhancement of optical absorption in thin-film silicon solar cells," *Plasmonics* **4**(2), 107–113 (2009).
11. Y. A. Akimov, W. S. Koh, and K. Ostrikov, "Enhancement of optical absorption in thin-film solar cells through the excitation of higher-order nanoparticle plasmon modes," *Opt. Express* **17**(12), 10195–10205 (2009).
12. L. Yang, Y. Xuan, and J. Tan, "Efficient optical absorption in thin-film solar cells," *Opt. Express* **19**(S5 Suppl 5), A1165–A1174 (2011).
13. B. P. Rand, P. Peumans, and S. R. Forrest, "Long-range absorption enhancement in organic tandem thin-film solar cells containing silver nanoclusters," *J. Appl. Phys.* **96**(12), 7519–7526 (2004).
14. M. Xue, L. Li, B. J. Tremolet de Villers, H. Shen, J. Zhu, Z. Yu, A. Z. Stieg, Q. Pei, B. J. Schwartz, and K. L. Wang, "Charge-carrier dynamics in hybrid plasmonic organic solar cells with Ag nanoparticles," *Appl. Phys. Lett.* **98**(25), 253302 (2011).
15. H. Shen, P. Bienstman, and B. Maes, "Plasmonic absorption enhancement in organic solar cells with thin active layers," *J. Appl. Phys.* **106**(7), 073109 (2009).
16. W. E. I. Sha, W. C. H. Choy, Y. P. Chen, and W. C. Chew, "Optical design of organic solar cell with hybrid plasmonic system," *Opt. Express* **19**(17), 15908–15918 (2011).

17. D. Qu, F. Liu, X. J. Pan, J. F. Yu, X. D. Li, W. L. Xie, Q. Xu, and Y. D. Huang, "Plasmonic core-shell nanoparticle enhanced optical absorption in thin film organic solar cells," presented at the 37th IEEE Photovoltaic Specialists Conference, Seattle, United States, 19–24 Jun. 2011.
 18. H. Hoppe, N. S. Sariciftci, and D. Meissner, "Optical constants of conjugated polymer/fullerene based bulk-heterojunction organic solar cells," *Mol. Cryst. Liq. Cryst. (Phila. Pa.)* **385**(1), 113–119 (2002).
 19. F. Monestier, J. J. Simon, P. Torchio, L. Escoubas, F. Flory, S. Bailly, R. de Bettignies, S. Guillerez, and C. Defranoux, "Modeling the short-circuit current density of polymer solar cells based on P3HT:PCBM blend," *Sol. Energy Mater. Sol. Cells* **91**(5), 405–410 (2007).
 20. A. D. Rakić, "Algorithm for the determination of intrinsic optical constants of metal films: application to aluminum," *Appl. Opt.* **34**(22), 4755–4767 (1995).
 21. E. D. Palik, *Handbook of Optical Constants of Solids* (Academic Press, Orlando, 1985).
 22. S. A. Maier, *Plasmonics: fundamentals and applications* (Springer, New York, 2007).
 23. F. J. Beck, A. Polman, and K. R. Catchpole, "Tunable light trapping for solar cells using localized surface plasmons," *J. Appl. Phys.* **105**(11), 114310 (2009).
-

1. Introduction

Utilizing metal nanoparticles (NPs) with plasmonic enhancement effect is considered as one of the promising methods for increasing the optical absorption of solar cells [1–17]. The metal NPs cannot only scatter and couple the incident light into the active layer [2–12] but also confine the light surrounding their surfaces [13–17], which results in the light absorption enhancement of solar cells. For different kinds of solar cell, the role of these two corresponding effects (i.e., surface plasmon enhanced scattering effect and localized surface plasmon (LSP) based field enhancement effect) in improving the light trapping should be different [1]. For silicon-based solar cells, the surface plasmon enhanced scattering effect dominates the optical enhancement, which had been demonstrated by our group and other researchers [2–12]. For thin film organic solar cells (OSCs), understanding which effect plays the dominant role is also important and helpful for us to make use of metal NPs based plasmonic enhancement effect to improve their efficiency.

In this paper, the optical absorption enhancement by plasmonic silver nanoparticles (Ag-NPs) in thin film OSCs has been studied theoretically based on the finite element method (FEM) with a three-dimension (3D) model. By depositing Ag-NPs at different positions of thin film OSCs, the enhancement mechanism is studied and discussed. The simulation results indicate that the LSP based field enhancement effect dominates the optical absorption enhancement in thin film OSCs with Ag-NPs, which is different from the effect for improving the efficiency of a-Si:H solar cells [12]. It is surprising that the plasmonic assisted optical absorption enhancement is the most significant when Ag-NPs are deposited at the interface of poly (3,4-ethylenedioxythiophene): poly (styrenesulfonate) (PEDOT:PSS) and poly (3-hexylthiophene): (6,6)-phenyl-C61-butyric-acid-methyl ester (P3HT:PCBM) layers rather than merely inserted into the P3HT:PCBM active layer of thin film OSCs. The absorption enhancement value could be higher than 100% owing to the whole spectrum enhancement with Ag-NPs at the interface of PEDOT:PSS and P3HT:PCBM layers of OSCs. In addition, the influence of Ag-NPs' diameter and spacing on the absorption enhancement has also been illustrated.

2. Plasmonic organic solar cell model

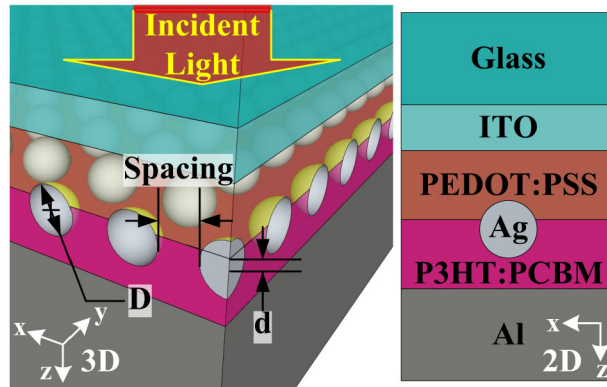


Fig. 1. Schematic diagram of thin film organic solar cell with Ag nanoparticles. On the left side shows the 3D image, while on the right side shows the 2D one.

As shown in Fig. 1, the thin film organic solar cell involved in this paper consists of a glass, a 20nm-thick indium tin oxide (ITO) layer, a 30nm-thick PEDOT:PSS anode layer, a 30nm-thick active layer of P3HT:PCBM with 1:1 weight ratio, and a 100nm-thick aluminum (Al) cathode. The plasmonic enhancement effect is studied by introducing the periodically distributed Ag-NPs inside the PEDOT:PSS layer, the P3HT:PCBM layer, and at the interface between PEDOT:PSS and P3HT:PCBM layers, respectively. The Ag-NPs with diameter D and spacing S has an offset d from the interface of PEDOT:PSS and P3HT:PCBM layers.

The 3D model of FEM is adopted to simulate the optical absorption of the structure shown in Fig. 1. Plane waves propagating along z -direction with unity amplitude are introduced at the top boundary. The periodic boundary condition in x and y direction is applied for considering the multiple scattering and cross-coupling between the neighboring nanoparticles. Herein, just one quarter of the period is concerned, which greatly decreases the computational complexity [4]. The details of the simulation method can be seen in Refs. 4, 9, 10, 11, and 15. The optical properties including the wavelength-dependent refractive index n and extinction coefficient k of ITO, PEDOT:PSS, P3HT:PCBM (1:1), Al, and Ag are taken from Refs. 18-21.

3. Results and discussions

Define the absorbed photon number spectrum ($APNS$) as

$$APNS(\omega) = A(\omega) \times AM(\omega) \quad (1)$$

where $AM(\omega)$ is the spectral photon number of the standard AM 1.5G shown as the red dotted line in Fig. 2, and $A(\omega)$ is the spectral absorption rate defined as the part of the incident spectral power absorbed in the active layer of solar cells [9].

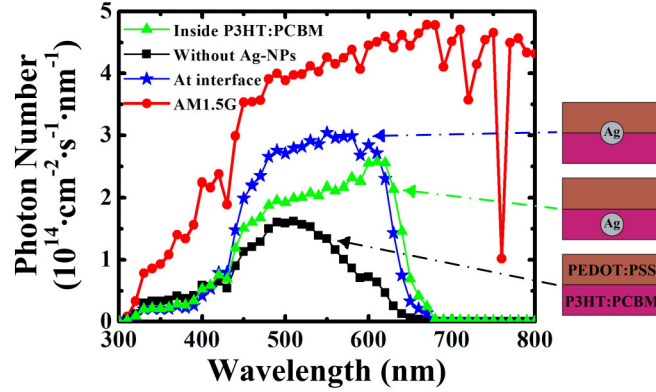


Fig. 2. Absorption photon number spectra of OSC without Ag-NPs (black square line), with Ag-NPs totally embedded in the P3HT:PCBM active layer (offset $d = 15\text{nm}$, green triangle line), and with Ag-NPs deposited at the interface of the PEDOT:PSS anode layer and the P3HT:PCBM active layer ($d = 0\text{nm}$, blue star line), respectively. The red dotted line indicates the photon number spectrum of the standard AM 1.5G. Here, diameter $D = 25\text{nm}$ and spacing $S = 15\text{nm}$.

Then, the absorbed photon number spectra of OSCs with and without Ag-NPs can be calculated and shown in Fig. 2. The black square line illustrates the photon number absorbed by the conventional thin film OSCs without Ag-NPs. By introducing the Ag-NPs (with diameter $D = 25\text{nm}$, spacing $S = 15\text{nm}$ and offset $d = 15\text{nm}$) inside the active layer of OSCs (P3HT:PCBM), it is illustrated that the green triangle line has an obvious enhancement compared with the black square line, which means more photons can be absorbed by the active layer with the help of Ag-NPs. If the Ag-NPs are located at the interface of PEDOT:PSS and P3HT:PCBM layers, it is surprising that the photon absorption (blue star line) is further increased compared with the green triangle line.

By defining the absorption enhancement (AE) as

$$AE \equiv \frac{\int APNS(\omega)_{With_Ag-NPs} d\omega - \int APNS(\omega)_{Without_Ag-NPs} d\omega}{\int APNS(\omega)_{Without_Ag-NPs} d\omega} \times 100\% \quad (2)$$

the green triangle line has an enhancement value of 73% compared to the black square line, and the absorption enhancement AE of the blue star line is as high as 106%.

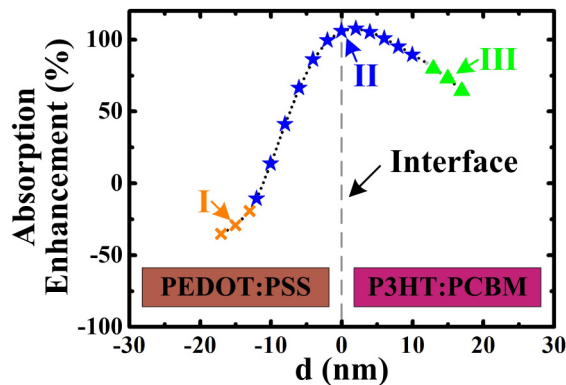


Fig. 3. Absorption enhancement (AE) as a function of the offset d for the OSCs with Ag-NPs. Here, diameter $D = 25\text{nm}$, spacing $S = 15\text{nm}$.

Further, with varying positions of Ag-NPs (offset d), the absorption enhancement as a function of the offset d is shown in Fig. 3. When Ag-NPs are embedded in the PEDOT:PSS layer (the orange cross points in Fig. 3), the light absorption efficiency is decreased (Absorption enhancement $< 0\%$). Namely, the Ag-NPs have a negative effect on increasing the light absorption of OSCs in this condition. When locating at the interface of PEDOT:PSS and P3HT:PCBM layers (the blue star points in Fig. 3), the Ag-NPs could effectively improve the light absorption of OSCs with absorption enhancement up to 106%, which is even higher than that when the Ag-NPs are totally embedded inside the P3HT:PCBM layer (the green triangle points in Fig. 3).

To understand the above phenomena and the mechanisms of plasmonic optical enhancement by metal NPs in OSCs, the distribution of electric field intensity in the OSCs has been studied. Meanwhile, since the light intensity of LSP surrounding the metal NPs is proportional to that inside the metal NPs [22], we propose to evaluate the light confined surrounding Ag-NPs by calculating the light confined inside the Ag-NPs, which can help us understand the role of LSP in improving the optical absorption of the P3HT:PCBM active layer. In this way, we can obtain the enhancement range and the peak wavelengths of the LSP based field enhancement effect in OSCs, and then analyze the role of LSP conveniently.

Figure 4(a) and the orange line in Fig. 5 correspond to the point I in Fig. 3 with Ag-NPs in the PEDOT:PSS layer. It is indicated that the LSP has been excited around $\lambda_0 = 450\text{nm}$ with Ag-NPs surrounded by PEDOT:PSS material, through observing the strong field intensity inside and outside Ag-NPs in Fig. 4(a) and the high optical absorption inside the Ag-NPs of the orange line in Fig. 5. Meanwhile, it can be found that the lower field intensity inside Ag-NPs does not always correspond to the lower field intensity outside Ag-NPs by taking a look at the case of 550-700nm, which results from the scattering effect of Ag-NPs. Since both the enhanced field excited by LSP resonance and the scattering field are almost concentrated in the PEDOT:PSS anode layer, the P3HT:PCBM active layer would absorb less incident light compared to the OSC without Ag-NPs, and the efficiency of the OSC with Ag-NPs in this situation would decrease. That is why the Ag-NPs inside the PEDOT:PSS layer have a negative effect on improving the efficiency of OSCs.

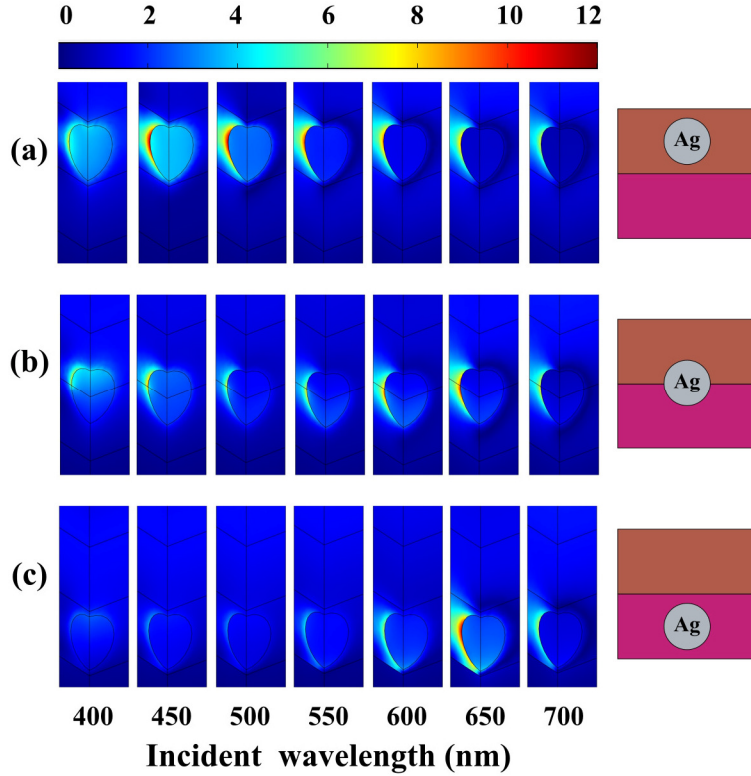


Fig. 4. Electric field distributions with Ag-NPs (diameter $D = 25\text{nm}$, spacing $S = 15\text{nm}$) (a) inside the PEDOT:PSS layer (offset $d = -15\text{nm}$), (b) at the interface of PEDOT:PSS and P3HT:PCBM layers ($d = 0\text{nm}$), and (c) inside the P3HT:PCBM layer ($d = 15\text{nm}$), respectively.

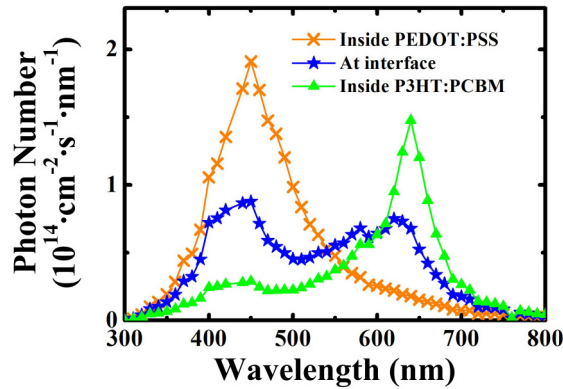


Fig. 5. Absorption photon number spectra of Ag-NPs inside the PEDOT:PSS layer (offset $d = -15\text{nm}$, orange line), at the interface of PEDOT:PSS and P3HT:PCBM layers ($d = 0\text{nm}$, blue line), and inside the P3HT:PCBM layer ($d = 15\text{nm}$, green line), respectively.

Figure 4(c) and the green line in Fig. 5 correspond to the point III in Fig. 3 with Ag-NPs in the P3HT:PCBM active layer. Since the resonance wavelength of LSP is related to the refractive index of dielectrics surrounding metal NPs [23], the peak wavelength moves from about $\lambda_0 = 450\text{nm}$ to 650nm when PEDOT:PSS is replaced by P3HT:PCBM with different material property. It is noticed that the lower field intensity inside Ag-NPs always

corresponds to the lower intensity outside Ag-NPs in this situation, which means that the scattering field is weak. Therefore, the enhanced field is mainly induced by LSP resonance, which improves the light absorption of the P3HT:PCBM active layer for generating electricity, especially near the peak wavelength (within the range of 550-700nm shown as the green triangle line in Fig. 2).

As different from the above two situations, when Ag-NPs are deposited at the interface of PEDOT:PSS and P3HT:PCBM layers, the LSP resonance can be excited not only in the short wavelength region (around $\lambda_0 = 450\text{nm}$) but also in the long wavelength region (around $\lambda_0 = 650\text{nm}$) due to the direct contact between the Ag-NPs and the two materials simultaneously. This is indicated by Fig. 4(b) and the blue line with two peaks of LSP resonance in Fig. 5. Although the excitation of LSP around $\lambda_0 = 450\text{nm}$ is related to non-active PEDOT:PSS layer, the field of LSP resonance could spread to the P3HT:PCBM active layer shown obviously in the Fig. 4(b) at $\lambda_0 = 450\text{nm}$ and 500nm . Therefore, the plasmonic enhancement has been extended to a wider spectrum (350-700nm), and the blue star line in Fig. 2 has a further enhancement in the short wavelength region compared with the green triangle line.

Actually, from the images of Fig. 4(a) and (b), we can observe the scattering field more or less. However, for the situation I and III in Fig. 3, there is limited help for improving the light absorption of OSCs with the scattering field in the above analysis. On the other hand, for the situation II in Fig. 3, there is obvious enhancement relative to LSP resonance. Considering the perfect match of the enhancement and the peak wavelength of LSP resonance in the situation III, it can be concluded that the LSP based field enhancement effect plays a dominant role in increasing the optical absorption when the metal NPs are introduced into the OSCs.

Furthermore, the structure parameters of diameter D and spacing S are varied to study the plasmonic absorption enhancement. Figure 6(a) and (b) show the absorption enhancement when Ag-NPs are deposited at the interface of PEDOT:PSS and P3HT:PCBM layers and totally embedded inside the P3HT:PCBM layer, respectively. By comparing the two images, it can be found that the absorption enhancement of OSCs with Ag-NPs at the interface are generally higher than that with Ag-NPs inside the P3HT:PCBM active layer, thanks to the two-peak LSP resonance effect.

By defining the D/S ratio as the ratio of the diameter D and spacing S of Ag-NPs, it is indicated that high absorption enhancement can be achieved when the D/S ratio is controlled within the two dashed lines for the two situations. In Fig. 6(a), the high enhancement value of above 80% can be easily obtained in a wide range of D/S ratio with Ag-NPs at the interface of PEDOT:PSS and P3HT:PCBM layers. And in Fig. 6(b), the enhancement value of above 60% can also be obtained with Ag-NPs inside the P3HT:PCBM active layer. As the optimized results, 108% (the white circle in Fig. 6(a)) and 75% (the red circle in Fig. 6(b)) are achieved. Therefore, introducing the Ag-NPs with certain diameter (within 10-28nm) and specific D/S ratio (about 1.1-3.8 and 1.1-2.2 for the two situations shown in Fig. 6(a) and (b), respectively) can improve the efficiency of OSCs effectively.

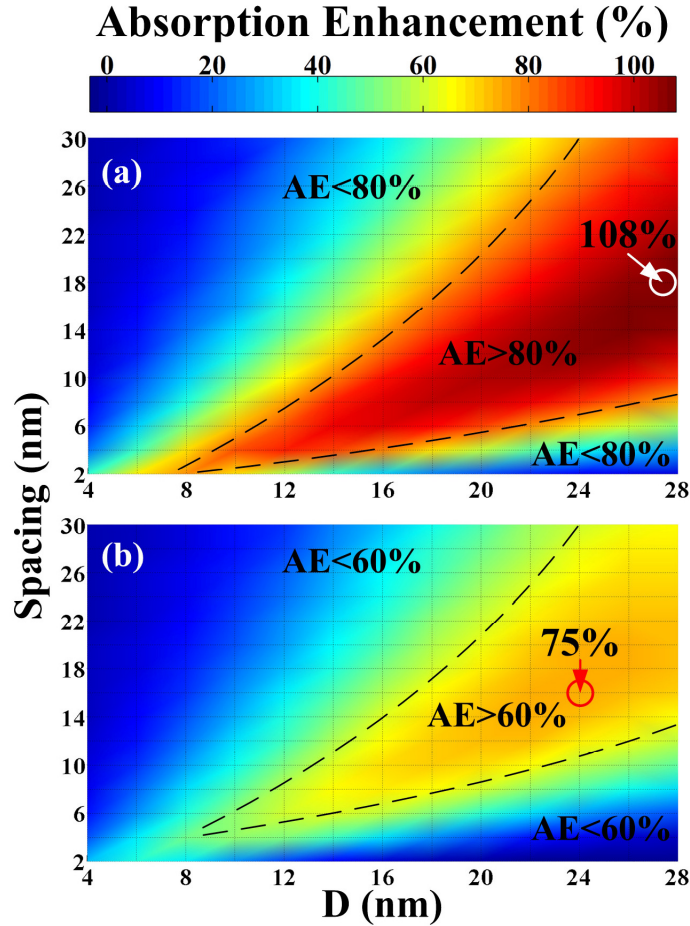


Fig. 6. Absorption enhancement (AE) as functions of the diameter D and spacing S of Ag-NPs when they are deposited (a) at the interface of PEDOT:PSS and P3HT:PCBM layers (offset $d = 0\text{nm}$) and (b) inside the P3HT:PCBM layer ($d = -15\text{nm}$), respectively.

4. Conclusion

The optical absorption enhancement by plasmonic metal NPs in thin film OSCs has been studied theoretically. Considering Ag-NPs at different positions of thin film OSCs, it is found that the LSP based field enhancement effect plays a dominant role in the optical absorption enhancement in thin film OSCs. By depositing the Ag-NPs at the interface of PEDOT:PSS and P3HT:PCBM layers, the plasmonic enhancement effect could be extended to a wider optical spectrum. The absorption enhancement value could be as high as 108%. Through varying the parameters of Ag-NPs, it is demonstrated that the enhancement with Ag-NPs at the interface is generally higher than that with Ag-NPs merely inside the active layer.

Acknowledgements

This work was supported by the National Basic Research Programs of China (973 Program) under Contract No. 2011CB301803 and No. 2010CB327405, the National High-tech R&D Program (863 Program) under Contract No. 2011AA050504, and the National Natural Science Foundation of China (NSFC-61036011, NSFC-61107050 and NSFC-60877023). The authors would like to thank Mr. Yoshiaki Oku, Mr. Dai Ohnishi and Mr. Hiroki Tsujimura of

ROHM Co., Ltd., as well as Prof. Jiangde Peng, Prof. Wei Zhang, Prof. Xue Feng, Dr. Kaiyu Cui, and Xujie Pan for their helpful comments.